A Study of the Formation of Molecular Sieve SAPO-44

Yining Huang,* David Machado, and Christopher W. Kirby

Department of Chemistry, The University of Western Ontario, London, Ontario, Canada N6A 5B7

Received: July 8, 2003; In Final Form: November 5, 2003

The formation of a silicoaluminophosphate-based molecular sieve SAPO-44 has been investigated in the present study. Particular attention was directed toward the characterization of the intermediate phases formed at different stages during the synthesis. The changes in the long-range ordering of the gel phases as a function of crystallization time was monitored by powder X-ray diffraction, and the development of the local structure of P, Al, and Si atoms was followed by ^{31}P, ^{27}Al, and ^{29}Si magic-angle spinning NMR. ^{1}H → ^{31}P cross polarization (CP) was employed to differentiate the P sites in different phases coexisting in the sample. Several ^{27}Al/^{31}P and ^{27}Al/^{29}Si double-resonance NMR experiments such as CP and transferred echo double-resonance were also utilized to identify the nature of the intermediate phases, and to select the P−O−Al and Si−O−Al bonding connectivities. FT-Raman spectroscopy was used to gain the information regarding the evolution of the porosity in the framework and the immediate environments around the template molecules. On the basis of the experimental results, a possible route for the formation of SAPO-44 is discussed.

Introduction

Microporous materials (often referred to as molecular sieves) are framework solids with pores, channels, and cavities with molecular dimensions. Perhaps, zeolites (that are aluminosilicates) are the best-known family of these materials. They are extensively used in industry for catalysis and separation.[1] Another important type of molecular sieves is the aluminophosphate (AlPO)-based material.[2] Some of these materials have the framework topologies of known zeolites, but many others have novel structures. These AlPO-based materials exhibit distinct molecular sieving characteristics. Since the frameworks of AlPOs are neutral, they usually have no inherent catalytic capabilities. However, they can be made catalytically active by introducing silicon into the framework. The resulting materials are so-called SAPOs (silicoaluminophosphates). Due to the potential and actual industrial applications, the synthesis of new microporous materials is one of the active areas in materials science. Although much data have been compiled on the synthesis conditions, the mechanisms of the crystallization are not well understood (ref 3 includes several reviews on microporous materials synthesis). Similar to zeolites, AlPOs and SAPOs are normally prepared under hydrothermal conditions. The processes involve the formation of intermediate gels. However, the structural properties of these gel phases are usually poorly understood. Because crystalline molecular sieves are eventually produced from these intermediate phases, the detailed knowledge of their structures is crucial to a better understanding of the self-assembly processes of the framework.

In the present study, we have investigated intermediate phases of molecular sieve SAPO-44. SAPO-44 is a small-pore silicoaluminophosphate-based molecular sieve with CHA structure (Figure 1).[4] It was first synthesized by Union Carbide in 1988.[5] The framework contains double six-membered rings (D6R) joined together through four-membered rings (4R). The resulting three-dimensional structure has large ellipsoidal cages that also

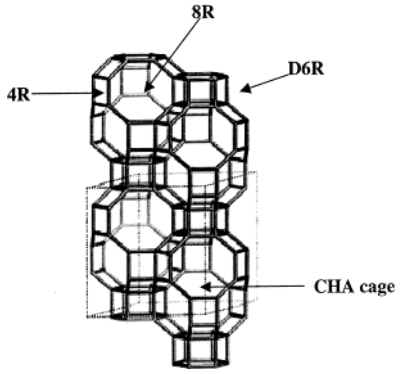

Figure 1. The framework structure of SAPO-44 (CHA). Four chabazite (CHA) cages are shown in the diagram.

are called the chabazite (CHA) cages. Small guest molecules can enter the cages through eight-membered ring (8R) windows. SAPO-44 and metal-substituted SAPO-44 molecular sieves are good catalysts for the alcohol-to-aliphatic hydrocarbon conversion reactions.[6] Similar to most AlPOs and SAPOs, SAPO-44 is also made under hydrothermal conditions from an initial gel formed upon mixing phosphoric acid, aluminum oxide, and silicon sources as well as template molecules (cyclohexylamine). There were several papers concerning the synthesis of SAPO-44 and metal-substituted SAPO-44, but the main emphasis was on the silicon/metal incorporation.[7] Only one report involved extensive examination of the intermediate phases by X-ray diffraction (XRD), simple magic-angle spinning (MAS) NMR, and other techniques.[7a] However, it is noted that in this study the gel samples were calcined at a high temperature (833 K) prior to characterization. Although SAPO-44 itself is stable at this temperature, the structures of the intermediate gel phases will inevitably be altered by calcination. Consequently, it would be difficult to directly correlate the properties of the calcined gel samples with the crystallization process. In this work, we have characterized intermediate phases of SAPO-44 synthesis (which were obtained by quenching the reaction at different times), using several solid-state NMR techniques in combination

* Author to whom correspondence should be addressed. E-mail: yhuang@uwo.ca.

10.1021/jp0308256 CCC: $27.50
Published on Web 01/17/2004

with powder XRD and FT-Raman spectroscopy. In particular, we have utilized ^{31}P, ^{27}Al, and ^{29}Si MAS NMR to probe the changes in coordination environments of P, Al, and Si atoms, ^{27}Al $\rightarrow$ ^{31}P cross polarization (CP) and ^{27}Al $\rightarrow$ ^{29}Si transferred echo double-resonance (TEDOR)[8] to select the ^{27}Al$-$O$-$^{31}P and ^{27}Al$-$O$-$^{29}Si connectivities in the intermediate gel phases, ^{1}H $\rightarrow$ ^{31}P CP to differentiate the P sites in different phases coexisting in the sample. Powder XRD was employed to follow the evolution of the long-range ordering, and FT-Raman was used to explore the development of the porosity and the interactions between the inorganic gel species and organic template.

Experimental Section

Hydrothermal synthesis of SAPO-44 was carried out using a procedure described by Ashtekar et al.[9] A typical preparation procedure was the following. Solution 1 was prepared by dissolving pseudo-boehmite [Catapal-B, (Vista, 65 wt % Al_2O_3)] and orthophosphoric acid (BDH, 85%) in water, and solution 2 was prepared by adding fumed silica (CAB$-$O$-$Sil, 99.8%) to a mixture of cyclohexylamine (Aldrich, 99+%) and water. Solution 2 was then added to solution 1 with vigorous agitation. Stirring of the resulting slurry for 2 h yielded a uniform and very viscous gel. The gel had a composition of $1.0Al_2O_3/1.0P_2O_5/1.0SiO_2/1.9R/63H_2O$ (R = cyclohexylamine). For each batch of preparation, a small portion of the gel was air-dried at room temperature, and this sample is referred to as initial gel without heating. The rest of the gel was then transferred to several stainless steel autoclaves and heated in an oven for various lengths of time at 190 °C. The reaction was quenched at different times by placing the autoclave in an ice bath, and the solid was then separated from the liquid phase by centrifugation. The solid materials were carefully dried in air at room temperature. All the gel samples were kept in tightly sealed glass vials after being dried. They were regularly checked by ^{31}P and ^{27}Al MAS NMR and powder XRD, and neither their MAS spectra nor the XRD patterns changed during the course of the work. The as-made SAPO-44 had an Al/P/Si ratio of 0.49:0.32:0.16, determined by a LEO440 scanning electron microscope (SEM) equipped with a Quartz Xone energy-dispersive X-ray (EDX) analysis system.

Powder X-ray diffraction patterns were recorded on a Rigaku diffractometer using Co Kα radiation (λ = 1.7902 Å) in a 2θ range of 5$-$65 degrees with a step-width of 0.05.

Raman spectra were obtained with a Bruker RFS 100/S FT-Raman spectrometer equipped with a near-infrared Nd:YAG laser operating at 1064 nm and a liquid nitrogen-cooled Ge detector. The resolution was 2 cm^{-1}.

NMR experiments were performed on a Varian/Chemagnetics Infinityplus 400 WB spectrometer equipped with three rf channels operating at the field strength of 9.4 T. The Lamar frequencies of ^{1}H, ^{31}P, ^{27}Al, and ^{29}Si were 399.9, 161.6, 104.1, and 79.8 MHz, respectively. Three NMR probes (a Varian/Chemagnetics 7.5-, and a 9.5-mm triple tuned MAS probe and a 3.2-mm double tuned probe) were employed, depending on the requirement of specific experiment. For the ^{31}P and ^{29}Si MAS experiments, the 7.5-mm probe was used with a spinning rate in the range 5$-$7 kHz. The pulse lengths of 3 and 3.6 μs were employed (the corresponding nominal 90° pulse lengths were 10 and 12 μs) for ^{31}P and ^{29}Si, respectively. The recycle delays were 90 s. The rf field strength for ^{1}H decoupling was around 60 kHz. The ^{27}Al MAS experiments were carried out using the 3.2-mm probe. The spectra were acquired by using short excitation pulses (typically less than 1.5 μs, corresponding to magnetization tip angles less than 10°). The rotor speed was in the 12$-$18 kHz regime and a pulse delay of 0.3 s was employed. Shift referencing was compared to 85% H_3PO_4, 1M $Al(NO_3)_3$ (aq), and TMS for ^{31}P, ^{27}Al, and ^{29}Si, respectively. The 7.5-mm probe was utilized for all the CP experiments. The ^{27}Al $\rightarrow$ ^{31}P cross polarization under MAS conditions was conducted in the sudden passage regime (i.e., weak, rf spin-locking field and fast sample spinning) because ^{27}Al (I = 5/2) is a quadrupolar nucleus.[10] The modified Hartmann$-$Hahn matching condition is

$$\gamma_P B_{1,P} = 3\gamma_{Al} B_{1,Al} \pm \nu_r$$

The spin-locking field strength for ^{27}Al was typically 15$-$21 kHz, corresponding to the ^{27}Al 90° pulse lengths between 17 and 12 μs measured for the central transition. The Hartmann$-$Hahn matching conditions were set on VPI-5 where optimized contact time of 1.5 ms was determined. A pulse delay of 0.1 s and a spinning rate of 7 kHz were typically used. The two-dimensional ^{27}Al $\rightarrow$ ^{31}P CP experiments were performed using the method described by Fyfe et al.[11] For ^{1}H $\rightarrow$ ^{31}P and ^{1}H $\rightarrow$ ^{29}Si CP experiments, the Hartmann$-$Hahn matching conditions were calibrated on the samples of ammonium dihydrogen phosphate and tetrakis(trimethylsilyl)silane for ^{31}P and ^{29}Si, respectively. Proton 90° pulse lengths were typically 5$-$8 μs and a pulse delay of 5 s was used. The ^{27}Al $\rightarrow$ ^{29}Si TEDOR experiments were carried out with the 9.5-mm probe. The sample was spun at 2.5 kHz. The pulse sequence employed was described in detail in ref 11. The ^{27}Al 90° pulse (central transition only) and ^{29}Si 90° pulse lengths were both set to be 12 μs. The number of rotor cycles before and after the coherence transfer were two and one, respectively, and they were experimentally optimized on zeolite Na-A.

Results and Discussion

Powder XRD Patterns. The powder XRD patterns of the gel samples heated for different times were recorded to obtain the information on the evolution of the long-range ordering of the intermediate phases as a function of crystallization time. The pattern of the initial gel without heating (Figure 2A) looked very similar to that (see Supporting Information) of the starting material, pseudo-boehmite, indicating that the vast majority of the aluminum source has not reacted. The XRD patterns of the gel samples heated under hydrothermal conditions for 1, 2, and 3 h looked identical. Figure 2B illustrates the powder pattern of the 2 h gel, which contains a very broad peak in the 2θ range of 20$-$40 degrees, indicating the formation of an amorphous material. The reflections due to pseudo-boehmite are still visible, but they became weaker, implying that a portion of the pseudo-boehmite has dissolved. Heating the gel for 4 h resulted in a powder pattern (Figure 2C) exhibiting three phases. A very broad diffraction profile between 20 and 40 degrees indicates the presence of a significant amount of amorphous material. Observation of four weak and broad reflections at about 16, 32, 44, and 58 degrees representative of pseudo-boehmite implies that there was still unreacted aluminum source in the sample. In addition, appearance of several sharp peaks signifies that a more crystalline phase was starting to form. The sharp reflections, however, do not coincide with those of crystalline SAPO-44, suggesting that a crystalline intermediate was emerging. Further increase in heating time to 6 h led to an increase in the intensities of the sharp reflections at the expense of the peaks due to both the amorphous phase and aluminum source as shown in Figure 2D. The peaks due to crystalline material do not match

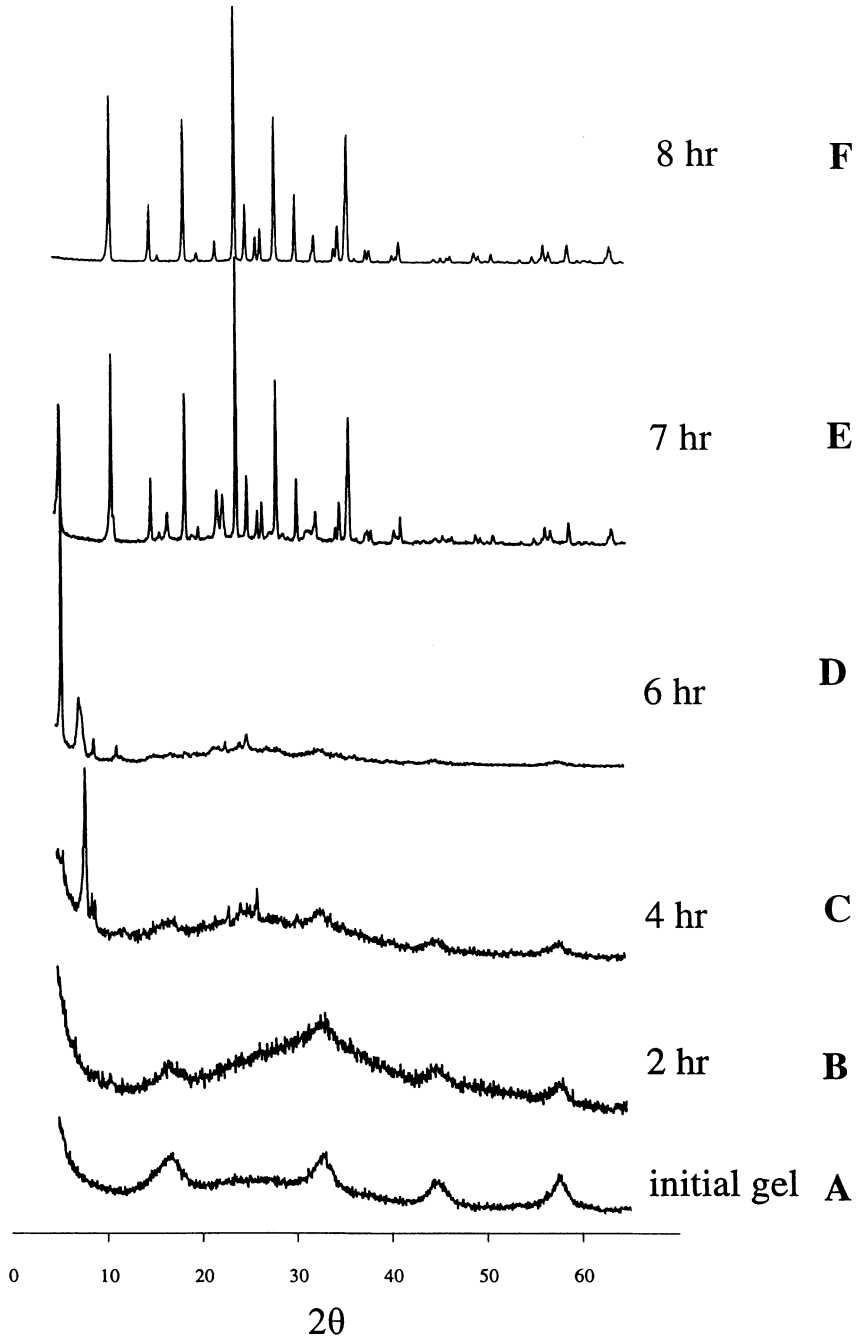

Figure 2. Powder XRD patterns of the selected gel samples.

any known AlPO-based molecular sieves, but the existence of several sharp low-angle peaks seems to indicate that this crystalline intermediate phase might have a layered structure. A scanning electron microscopic study also suggested the formation of layered materials as an intermediate.[7b] The XRD pattern of the 7 h gel shows the coexistence of both the layered intermediate and crystalline SAPO-44 molecular sieve (Figure 2E). Heating the gel for 8 h or longer yielded XRD patterns identical to pure crystalline SAPO-44 (Figure 2F).

The XRD patterns suggest that the formation of SAPO-44 under hydrothermal conditions occurs, at least, in three stages. The first stage appears to be predominantly the formation of an amorphous phase during the first 3 h of heating. The second step is the conversion of the amorphous material to a seemingly layered structure after heating the gels for 4−7 h. The final stage is the transformation of the layered material into the crystalline SAPO-44 molecular sieve, which starts occurring after 6 h of heating. Although the powder patterns have indeed furnished valuable information regarding the evolution of the long-range ordering of the gel samples, XRD gives neither indication on the nature of the intermediate phases (i.e., whether they are purely phosphate, aluminophosphate, or silicoaluminophosphate), nor the information on the local structure of P, Al, and Si.

^{31}P MAS Spectra. To gain a better understanding of the development of the local environments of P and Al atoms in the intermediate phases, we also carried out the ^{31}P and ^{27}Al MAS NMR experiments. The ^{31}P MAS NMR spectra of the initial gel without heating and the gel sample heated for 1 h both exhibit an asymmetric peak positioned at around −11 ppm (Figures 3A,B). This resonance is extremely broad with full width at half-height (fwhh) being 2.8 kHz. The broadness of the peak clearly indicates that the gel samples are amorphous in nature. In the previous studies of synthesis of AlPO-based

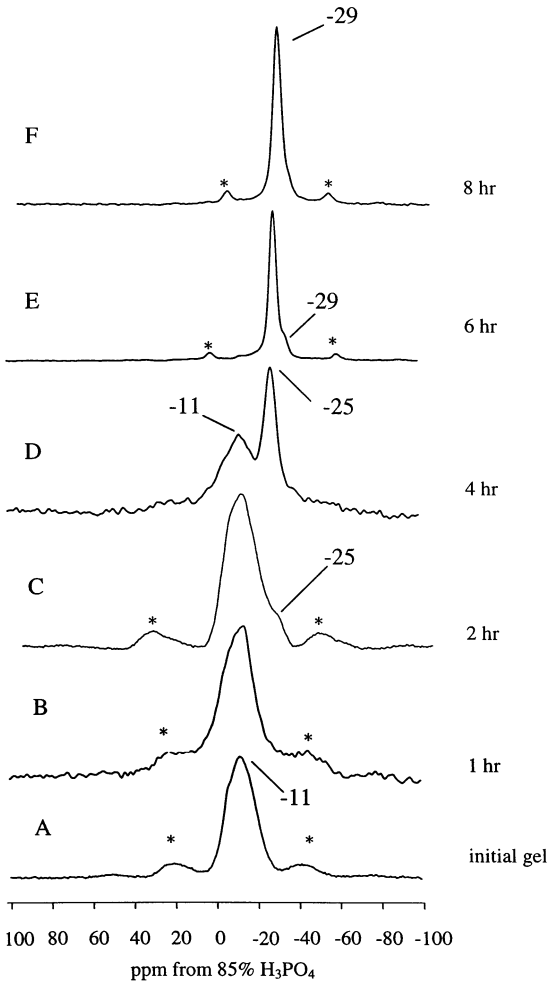

Figure 3. ^{31}P MAS spectra of the selected gel samples. Spinning sidebands are labeled with an asterisk.

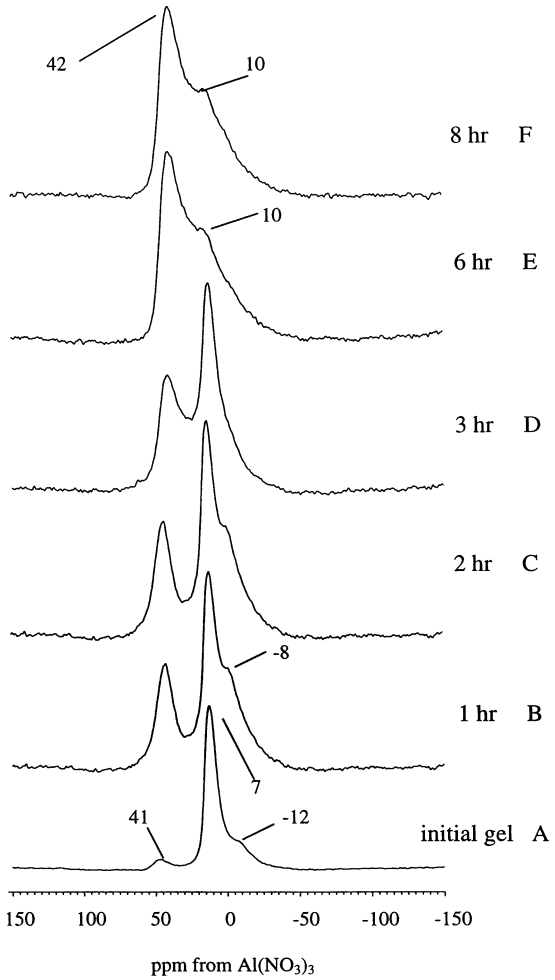

Figure 4. ^{27}Al MAS spectra of the selected gel samples.

microporous materials, a broad ^{31}P peak was often observed in the range −10 to −20 ppm for the gel samples obtained in the early stages of the crystallization,[12] and they are usually assigned to the P sites in the amorphous aluminophosphate materials. Thus, this resonance might be attributed to the tetrahedral P sites in the AlPO species. However, the ^{31}P chemical shifts of some simple phosphates and polyphosphates also appear in this region.[13] Therefore, the exact nature of this resonance cannot be assigned unambiguously without further experiments. For the sample heated for 2 h, its ^{31}P spectrum (Figure 3C) shows that in addition to the broad resonance at −11 ppm, a new peak starts emerging as a weak shoulder at about −25 ppm. The early work has established that ^{31}P chemical shifts of AlPO-based porous materials usually fall in the range between −19 and −31 ppm[14] and the peaks in this region are due to P atoms tetrahedrally bound to four Al atoms through bridging oxygen atoms. Therefore, the emergence of the new resonance at −25 ppm indicates the development of a new P site with $P(OAl)_4$ environment. But it is unclear whether this new P peak belongs to the same amorphous material or a different AlPO species. The ^{31}P spectrum (Figure 3D) of the sample heated for 4 h shows that the peak at −25 ppm has grown considerably at the expense of the signal at −11 ppm, which coincides with the appearance of the sharp reflections in the corresponding XRD pattern. Heating the initial gel for a period of 6 h resulted in a relatively sharp peak −25 ppm with a weak shoulder at ca. −29 ppm (Figure 3E). The spectrum of the 8-h gel looked identical to that of pure crystalline SAPO-44 and contains a single resonance at −29 ppm (Figure 3F).

^{27}Al MAS Spectra. Selected ^{27}Al MAS NMR spectra are shown in Figure 4. The spectrum of the initial gel without heating (Figure 4A) shows a very weak peak at 41 ppm and a strong peak at 7 ppm along with a weak shoulder at about −12 ppm. The weak peak at 41 ppm falls within the range of 35−48 ppm reported in the literature for tetrahedral Al environments of $Al(OP)_4$ for most microporous AlPO materials.[14] However, the assignments of the strong peak at 7 ppm and its shoulder at −12 ppm are not unambiguous. There are several possibilities that might be responsible for these resonances. The very strong peak at 7 ppm may be due to the unreacted Al source, since the ^{27}Al MAS spectrum of pseudo-boehmite displays a single resonance at 10 ppm (see Supporting Information). The spectrum is also consistent with the corresponding XRD pattern (Figure 2A), which exhibits the reflections of pseudo-boehmite. A previous study of the gel sample of SAPO-44 synthesis, however, assigned the resonance at around 7 ppm exclusively to five-coordinated Al sites in the AlPO species.[7a] On the basis of its shift value, the weak shoulder at −12 ppm may be attributed to the octahedral Al atoms in an AlPO species.[14] But several forms of alumina can also exhibit a broad signal in the region 40 to −20 ppm. It is known that the Al source can reprecipitate as aluminum oxide in different forms during molecular sieve crystallization.[15] Clearly, further experiments are needed to clarify the above-mentioned situations. Four initial gel samples were prepared by four separate experiments to examine the sample reproducibility. The XRD patterns and ^{31}P

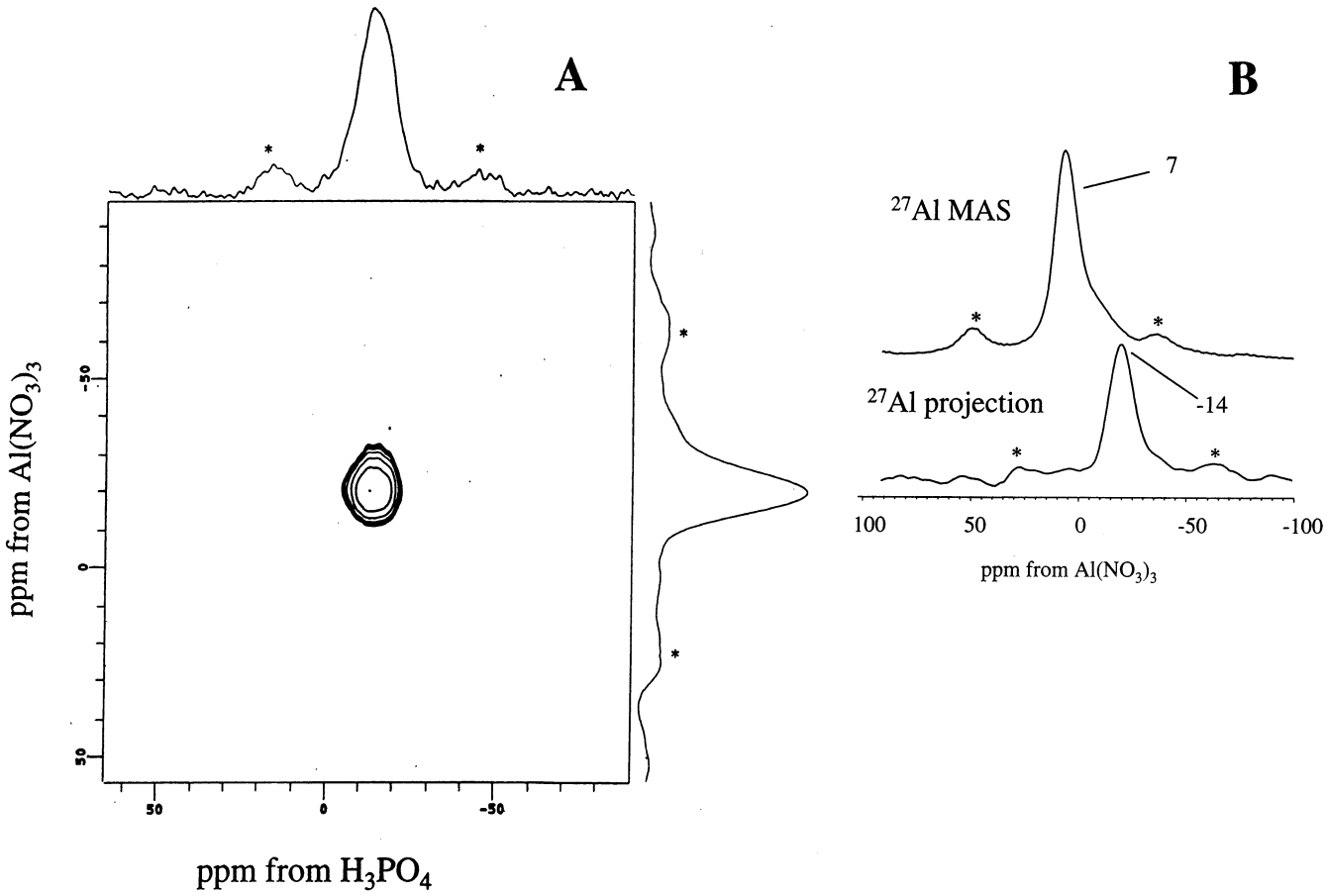

Figure 5. Initial gel without heating: (A) ^{27}Al → ^{31}P HETCOR spectrum with a contact time of 1 ms. For each of the 64 experiments in t_1, 26 000 scans were acquired. The pulse delay was 0.1 s, resulting in a total experimental time of 47.9 h. (B) ^{27}Al MAS spectrum (top) and ^{27}Al projection (bottom). Spinning sidebands are labeled with an asterisk.

MAS NMR spectra of all four gel samples were identical. The ^{27}Al MAS spectra of the samples from two batches are identical to Figure 4A, and the spectra of the other two samples (Figure 5B) also looked very similar to Figure 4A except that they did not contain the weak peak at 41 ppm, which implies that the reaction under ambient conditions does not produce large amounts of tetrahedral Al sites. Whether or not a small amount of tetrahedral Al will form may depend on other factors such as agitation. The spectra (Figures 4B,C) of the gel samples heated for 1 and 2 h also contain the three signals similar to those of the initial gel. However, the peak at 41 ppm has grown intensely with respect to the other two, suggesting a large amount of tetrahedral Al sites were produced as soon as hydrothermal treatment began. The shielded shoulder has also gained intensity significantly and shifted slightly from −12 to −8 ppm. For the gel heated for 3 h, its spectrum contains essentially two peaks at 42 and 7 ppm (Figure 4D). The shoulder observed at around −8 ppm in Figures 4B,C almost disappeared. Heating the gel for 6 h or longer yielded identical spectra (Figures 4E,F), which exhibit a broad asymmetric profile with two maximums at 42 and 10 ppm. It is not clear, however, whether the two maximums are due to two overlapping peaks or just a single resonance with an asymmetric line-shape resulting from an Al site with a large quadrupolar coupling constant.

^{27}Al → ^{31}P HETCOR Spectra. From the above discussion, it is apparent that despite the fact that the straightforward MAS spectra indeed provide invaluable information regarding the local environments of P and Al atoms, ambiguities do exist in identifying the nature of the intermediate phases and the spectral assignments. Much of the problem arises from the fact that the simple ^{31}P and ^{27}Al MAS experiments do not provide information on connectivity between Al and P atoms. To better characterize the gel phases and derive the information on bonding connectivity, we further carried out the ^{27}Al → ^{31}P cross polarization. CP process is mediated by heteronuclear dipolar coupling.[16] Because the strength of dipolar interaction is strongly dependent on the internuclear distance, CP spectra can yield information on connectivity between two unlike spins involved. In the case of ^{27}Al → ^{31}P CP, only the ^{31}P nuclei that are in the close vicinity of Al atoms will be detected, and consequently this approach can be utilized to select P−O−Al linkage in AlPO-based materials.[11] In the present study, we have used heteronuclear chemical shift correlation spectroscopy (HETCOR),[17] a two-dimensional (2D) technique based on CP to map out connectivity between Al and P in the gel samples. We first examined the initial gel without heating. As mentioned earlier, the nature of the peak at 7 ppm and its shielded shoulder at −12 ppm seen in the ^{27}Al MAS spectrum is not unambiguous. We examined the sample whose ^{27}Al MAS spectrum only exhibits two signals (the 7 ppm peak with a shoulder at −12 ppm) in question. The HETCOR spectrum (Figure 5A) illustrates that the P projection contains only a single resonance at −11 ppm corresponding to the only P peak observed in the ^{31}P MAS spectrum. The HETCOR spectrum clearly demonstrates that this phosphorus is connected to an aluminum site. The ^{27}Al projection shows that this Al resonance is at around −14 ppm, which coincides with the weak shoulder on the shielded side of the 7 ppm main peak seen in the MAS spectrum (Figure 5B). This signal can now be assigned unambiguously to the

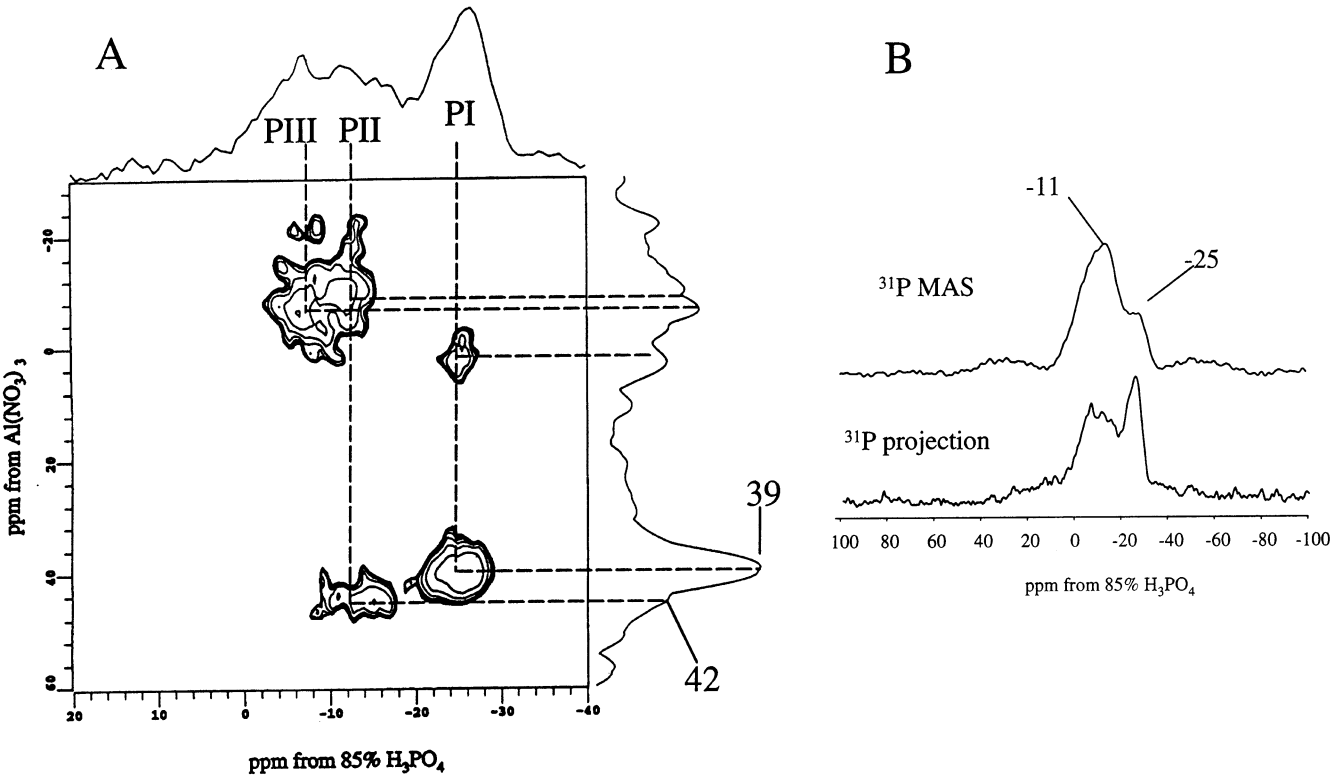

Figure 6. 2 h gel: (A) $^{27}Al \rightarrow {}^{31}P$ HETCOR spectrum with a contact time of 1 ms. For each of 64 experiments in t_1, 12 000 scans were acquired. The pulse delay was 0.1 s, resulting in a total experimental time of 22 h. (B) ^{31}P MAS spectrum (top) and ^{31}P projection (bottom).

octahedral Al site in the amorphous AlPO material. The very strong peak positioned at 7 ppm did not appear in the Al projection (Figure 5B), indicating that this resonance is not connected to any P. The result clearly indicates that the 7 ppm peak does not arise from five-coordinated Al in an AlPO species as suggested previously[7a] and therefore must be due to the unreacted Al source which is not expected to be connected to P. Observation of Al−O−P connectivity suggests that there was definitely a small amount of amorphous AlPO material starting to form before hydrothermal treatment began.

The 2 h gel sample was also investigated. This is the gel sample whose ^{31}P MAS spectrum shows a broad asymmetric peak at −11 ppm with a weak shielded shoulder at −25 ppm. Its HETCOR spectrum (Figure 6A) unveils three phosphorus sites, which have different connectivities to various Al sites. The first site (PI) corresponding to the shoulder at −25 ppm seen in ^{31}P MAS spectrum now appears as a well separated peak in the P projection. It strongly correlates to a tetrahedral Al site at 39 ppm. The correlation between this ^{31}P signal and a weak ^{27}Al resonance at approximate 0 ppm is also visible, suggesting that this phosphorus site is also connected to a small number of pentacoordinated aluminum atoms. The second P site (PII) appears at around −12 ppm, and this site is connected to an octahedral Al at −12 ppm and a tetrahedral Al site at 42 ppm. From the HETCOR spectrum it is also evident that the PI and PII sites correlate to two tetrahedral Al peaks with slightly different shifts. The third site (PIII) is positioned at about −6 ppm, and this site is linked solely to octahedral Al. As stated earlier, previous work has shown that for most of the microporous AlPO materials ^{31}P peaks with chemical shifts in the range of −19 to −31 ppm are usually due to the P atoms tetrahedrally bound to four Al atoms via bridging oxygen.[14] Therefore, the PI site represents fully condensed P with $P(OAl)_4$ environment. The CP result further implies that this phosphorus site has both tetrahedral and pentacoordinated Al in its second coordination sphere, $P[OAl(tet)]_x[OAl(pen)]_{(4-x)}$. The chemical shifts of PII and PIII are outside the range mentioned above, indicating that the number of Al in second coordination sphere for these sites are less than four. Observation of the Al−O−P linkages suggests that the number of Al atoms in the second coordination sphere is two or three for PII and one to three for PIII. Sayari et al. have suggested that the presence of hydroxyl groups directly attached to a P atom (P−OH) in AlPO materials induces a deshielded shift from the phosphorus with $P(OAl)_4$ environment.[14a] On the basis of their argument and the correlation map shown in Figure 6A, we conclude that the chemical environments are $P(OH)_x[OAl(oct)]_{4-x}$ ($1 \leq x \leq 3$) and $P(OH)_x[OAl(tet)]_y[OAl(oct)]_{4-(x+y)}$ ($x = 1$ or 2) for PIII and PII sites, respectively. Additional evidence supporting these assignments is that compared to the shoulder in the ^{31}P MAS spectrum, the intensity of PI site at −25 ppm observed in the ^{31}P projection was markedly enhanced relative to the peaks due to PII and PIII (Figure 6B). Fyfe et al. have carried out the $^{27}Al \rightarrow {}^{29}Si$ CP on various zeolites and found that the relative enhancement of Si signals could be related to the number of Al atoms in neighboring T sites (T = Al and Si).[18] In the present case, the enhancement of the ^{31}P resonance at −25 ppm is consistent with the argument that −25 ppm peak is due to fully condensed $P(OAl)_4$ environment experiencing a larger Al−P dipolar interaction resulting from a lager number of Al atoms in the second coordination sphere, whereas PII and PIII are due to partially condensed P sites (where the number of Al atoms in the second coordination sphere is less than 4). Again, the strongest peak at 7 ppm in the ^{27}Al MAS spectrum did not show up in the Al projection, confirming that it is due to Al source.

$^{1}H \rightarrow {}^{31}P$ CP Spectra. Although $^{27}Al \rightarrow {}^{31}P$ HETCOR spectrum revealed additional information on the local structure of Al and P atoms, it did not give any indication on whether

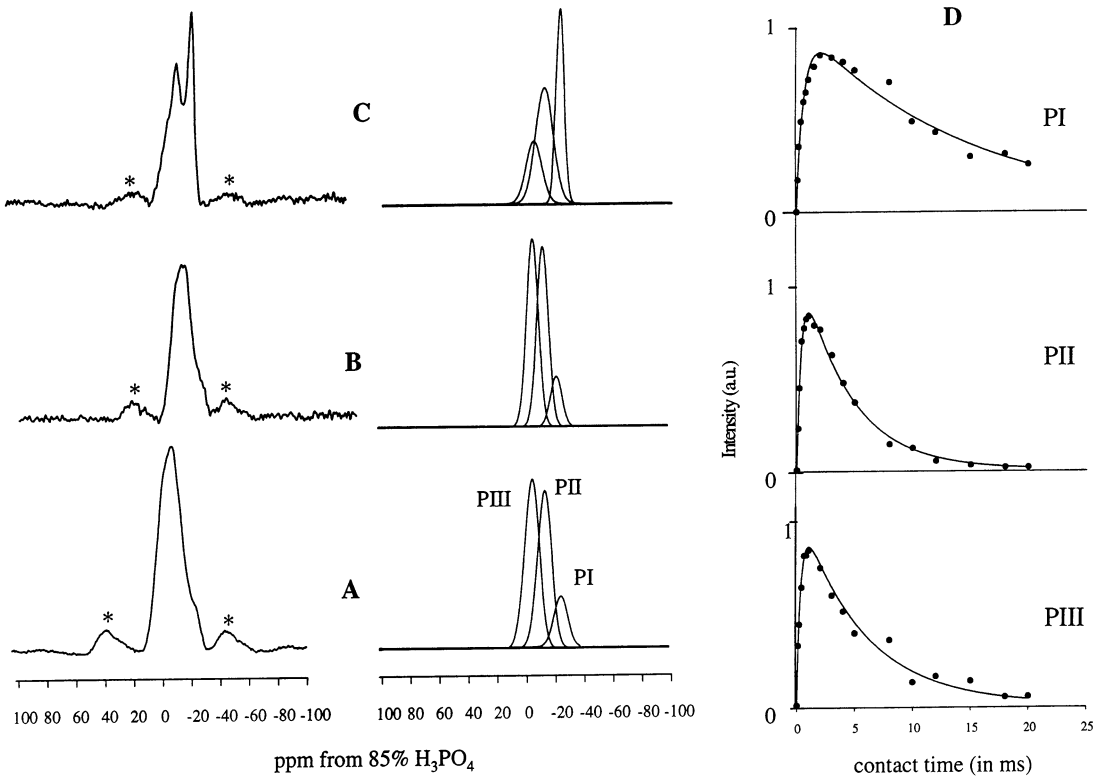

Figure 7. 2 h gel: (A) ^{31}P MAS spectrum. ^{1}H → ^{31}P CP spectra with contact time of (B) 0.1 ms and (C) 10 ms. Spinning sidebands are labeled with an asterisk. (D) Variation of the CP intensities as a function of contact time.

the three P sites are within the same amorphous material or belong to different phases. To shed some light on this question we further performed ^{1}H → ^{31}P CP experiments on 2 h gel sample. Figures 7A−C shows selected CP spectra with different contact times together with corresponding MAS spectrum for comparison. Each deconvoluted spectrum displays three peaks at −4, −10, and −25 ppm, coinciding with the peaks seen in the ^{27}Al → ^{31}P HETCOR spectrum at −6, −10, and −25 ppm, respectively. The spectrum with a short contact time of 0.1 ms (Figure 7B) looked similar to the corresponding MAS spectrum (Figure 7A). However, the long contact time (10 ms) discriminates against the peaks at −4 and −10 ppm (Figure 7C). Additional information regarding the observed discrimination may be obtained by examining the cross polarization dynamics. For each P site, the plots of the CP intensity as a function of contact time are shown in Figure 7D. The CP dynamics can be described by the equation

$$S(t) = S_{max}(1 - T_{CP}/T_{1\rho}{}^{H})^{-1}(\exp(-t/T_{1\rho}{}^{H}) - \exp(-t/T_{CP}))$$

The initial growth of CP signal is controlled by cross-polarization time constant, T_{CP}, which is related to the second moment of the dipolar interaction between two unlike spins. The exponential decay of the signal at longer contact times is determined by proton spin−lattice relaxation time in the rotating frame of reference, $T_{1\rho}{}^{H}$. By fitting the CP data to the above equation, the $T_{1\rho}{}^{H}$ and T_{CP} values can be estimated. The $T_{1\rho}{}^{H}$ values are 5, 4.2, and 14.3 ms and T_{CP} values 0.34, 0.39, and 0.64 ms for PIII, PII, and PI sites, respectively. Apparently, the selectivity seen in the CP spectra at a long contact time (Figure 7C) is the result of the differences in $T_{1\rho}{}^{H}$. It is known that a homogeneous domain tends to possess a single $T_{1\rho}{}^{H}$ value because of spin diffusion and in a heterogeneous system different domains (or phases) have different $T_{1\rho}{}^{H}$ values.[19] The fact that the values of $T_{1\rho}{}^{H}$ for PII (5.0 ms) and PIII (4.2 ms) are very similar, but differ remarkably from that of PI (14.3 ms), indicates that PII and PIII sites both exist in the same phase and PI likely belongs to a different domain. To further assist in interpretation of the CP data, we also carried out ^{1}H → ^{31}P CP on as-made SAPO-44 and the sample of initial gel without heating. From the CP dynamic curves (see Supporting Information), we obtained $T_{1\rho}{}^{H}$ values of 5.3 and 20.8 ms, and T_{CP} values of 0.55 and 2.34 ms for the initial gel and as-made SAPO-44, respectively. Apparently, the P resonance of the amorphous material in initial gel sample has a $T_{1\rho}{}^{H}$ value almost identical to that of the PII and PIII sites in the 2 h sample, confirming that the PII and PIII sites belong to the same phase which is amorphous in nature. Since the $T_{1\rho}{}^{H}$ value of PIII is much closer to that of crystalline as-made SAPO-44 than amorphous phase, this site likely belongs to an intermediate phase, which is more crystalline in nature. We further assign this peak to the P site of the layered material. However, the XRD patterns of the gel samples heated for less than 4 h did not show the reflections of this layered intermediate phase. It appears that heating the gel for 2 h starts yielding some very small crystallites of the layered material whose sizes are too small to be detected by X-ray diffraction. It is also worth noting that compared to the crystalline material, the P sites of amorphous material have smaller T_{CP} values, indicating the stronger P−H dipolar interactions. This is consistent with the suggestion that the PII and PIII sites are not fully condensed and have directly attached OH groups.

^{29}Si MAS, ^{1}H → ^{29}Si CP, and ^{27}Al → ^{29}Si TEDOR Spectra. ^{29}Si MAS spectra were obtained to monitor the incorporation of silicon atoms into the framework (Figure 8). The spectra of the initial gel without heating and the 2 h gel both display just a single peak at −110 ppm (Figures 8A,B), which can be assigned to the starting amorphous silica with a $Si(OSi)_4$ environment.[20] The result indicates that after 2 h of hydrothermal treatment, silicon atoms still have not been incorporated into

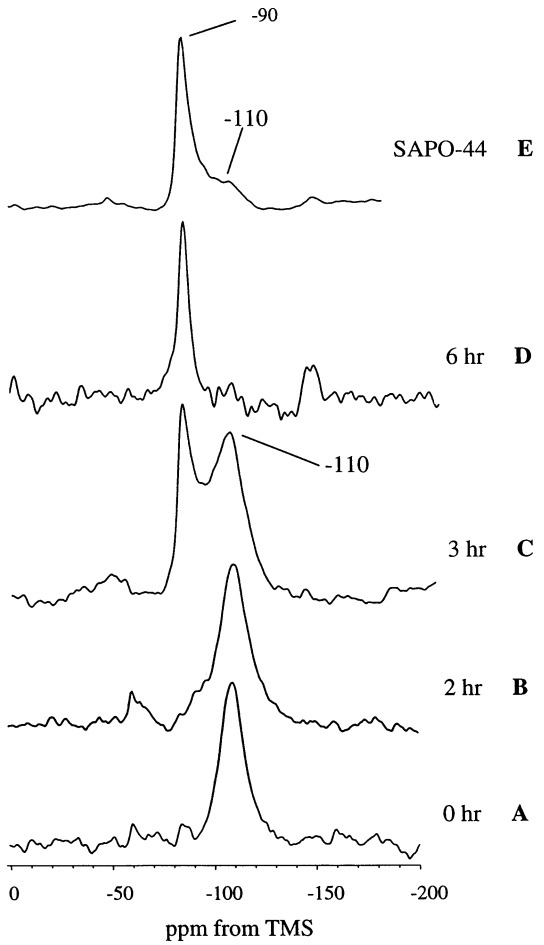

Figure 8. ^{29}Si MAS spectra of the selected gel samples.

any of the AlPO materials existing in the sample. When heating the gel for 3 h, a new peak at −90 ppm appeared (Figure 8C). With increasing heating time, this peak has grown in intensity at the expense of the peak at −110 ppm and after 6 h of heating the −110 ppm peak disappeared completely (Figure 8D). A ^{29}Si peak at around −90 ppm has been previously reported in a number of SAPO-based molecular sieves[21] including SAPO-44.[7] This peak has been previously attributed to a $Si(OAl)_4$ environment on the basis of the chemical shift value. Fyfe et al. were able to directly confirm this assignment for SAPO-37 by using ^{27}Al → ^{29}Si coherence transfer experiment.[22] We also assign the −90 ppm peak observed in as-made SAPO-44 (Figure 8E) to a $Si(OAl)_4$ environment. However, the nature of the same peak observed in the intermediate gel phases such as the sample heated for 3 h cannot be unambiguously assigned without further experiments because in addition to $Si(OAl)_4$ coordination, the $Si(OSi)_2(OH)_2$ environments in silica gel could also give rise to a peak at around −90 ppm[20] and existence of such local structure certainly is possible under the reaction conditions. The situation is further complicated by the ^{1}H → ^{29}Si CP spectra (Figures 9A−C), which shows that short contact times clearly discriminate in favor of the −90 ppm. This seemed to imply a stronger proton−silicon dipolar interaction experienced by the Si site at −90 ppm, which would be consistent with the possibility of existing $Si(OSi)_2(OH)_2$ environments. To ambiguously determine the nature of the −90 ppm resonance in 3 h gel, we performed ^{27}Al → ^{29}Si TEDOR experiments. As CP, TEDOR is also a coherence transfer technique designed to measure the weak heteronuclear dipolar couplings.[8] The reason for choosing this particular method is that previous work has demonstrated that among several commonly used dipolar coupling-based double-resonance experiments TEDOR seems to be the most efficient for studying ^{27}Al−O−^{29}Si connectivity in zeolitic materials.[18] The efficiency is extremely important in the present case because of the very low chemical content of silicon in the gel samples coupled with the low natural abundance of ^{29}Si (4.7%). Figure 9E illustrates the ^{27}Al → ^{29}Si TEDOR spectrum of 3 h gel sample, which contains a single resonance at −90 ppm. Observation of the −90 ppm peak in the TEDOR spectrum shows unambiguously that the origin of this peak is due to $Si(OAl)_4$ rather than $Si(OSi)_2(OH)_2$ environments. The peak at −110 ppm seen in the MAS spectrum did not appear in the TEDOR spectrum, confirming that this peak indeed originates from unreacted silica. In the MAS spectrum of as-made SAPO-44 (Figure 8E), there is a very broad weak shoulder with a maximum at around −110 ppm, corresponding to small silicon patches in the framework as reported by several workers.[6a,b,7a,c−d,f]

^{31}P → ^{27}Al CP Spectrum. Even though the aim of the work is to characterize the structure of the gel phases, the ^{27}Al MAS spectrum (Figure 3F) of as-made SAPO-44 is worth a few comments. The ^{27}Al MAS spectrum obtained at a spinning rate of 6 kHz (see Supporting Information) shows a very strong tetrahedral Al peak at 42 ppm and a broad resonance at around 10 ppm with a number of spinning sidebands, indicating that the second peak has a larger anisotropy. When spinning at 16 kHz (Figure 3F), the intensity of the broad peak at 10 ppm grew significantly. This broad peak was also seen in the ^{27}Al MAS spectra of SAPO-44 reported in the literature.[6d,7a,c−d] This peak was either interpreted as pentacoordinated Al in the SAPO-44 framework[7a] or left without comments.[6d,7c−d] We also noticed that the shift of this peak is typical of the octahedral Al in amorphous alumina. To identify the exact nature of this broad peak, we carried out 1D ^{31}P → ^{27}Al CP on as-made SAPO-44. This 1D experiment is equivalent to a 2D ^{27}Al → ^{31}P CP experiment because there is only one P signal and therefore any observed ^{27}Al CP signal must be coupled to the same P resonance. The ^{31}P → ^{27}Al CP spectrum (Figure 10B) shows a strong tetrahedral Al peak at 41 ppm, confirming that this Al is connected to the P. The broad peak at 10 ppm seen in Figure 3F now appeared in the CP spectrum as an extremely weak shoulder, indicating that the vast majority of the Al contributing to the 10 ppm peak seen in the MAS spectrum are due to amorphous alumina. However, a very small amount of pentacoordinated Al also exists.

FT-Raman Spectra. To obtain the information on the evolution of pore openings we also measured FT-Raman spectra (Figure 11). Early work has established that the frequency of the T−O−T bending mode (T = Al and Si) due to zeolite framework can be correlated to the average T−O−T angle and therefore the ring system in a zeolite.[23] Holmes et al. studied the Raman spectra of a number of AlPO-based molecular sieves and found that the breathing mode of the largest ring in the framework appears in the frequency range 100−350 cm^{-1}.[24] They further established an empirical correlation between the frequency of this "pore breathing" mode (ν) and the average Al−O−P angle (θ) around the unidimensional channel:

$$\cos\theta = 3.696 \times 10^{-6}\,\nu^2 - 1.102$$

The FT-Raman spectrum of calcined SAPO-44 (template free) shows that there is only a single peak at 247 cm^{-1} in the region of 100−350 cm^{-1}. From the XRD data of Bennett and Marcus,[4] the average T−O−T angle around the eight-membered ring of SAPO-44 (the largest pore in CHA structure) was calculated to

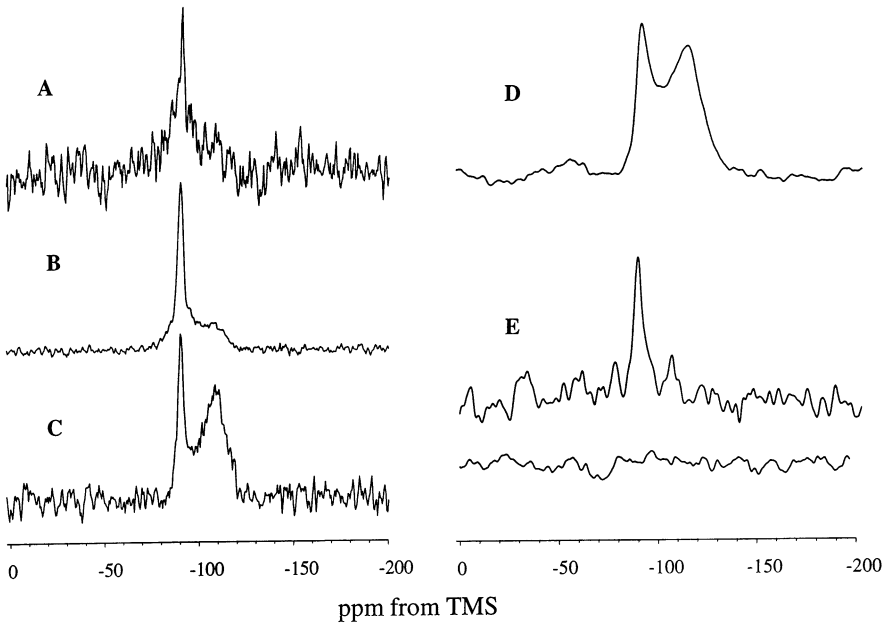

Figure 9. 3 h gel: $^{1}H \rightarrow {}^{29}Si$ CP spectra with contact time of (A) 0.1 ms, (B) 4 ms, and (C) 10 ms. (D) ^{29}Si MAS spectrum. (E) $^{27}Al \rightarrow {}^{29}Si$ TEDOR signal with the null experiment shown below. 2 200 000 scans were acquired and the pulse delay was 0.1 s. The null experiment was performed under the identical conditions except the ^{27}Al 90° coherence transfer pulse being removed.

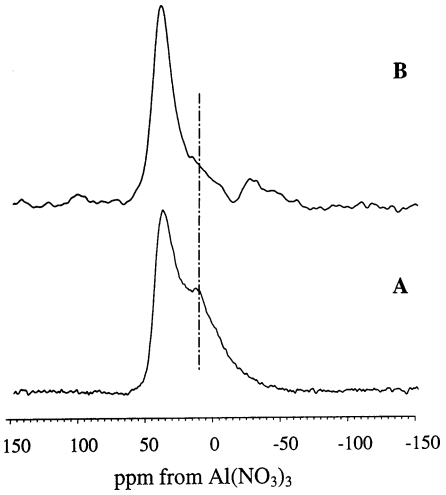

Figure 10. As-made SAPO-44: (A) ^{27}Al MAS spectrum. (B) $^{31}P \rightarrow {}^{27}Al$ CP spectrum acquired after 320 scans with a pulse delay of 240 s. The contact time was 1 ms.

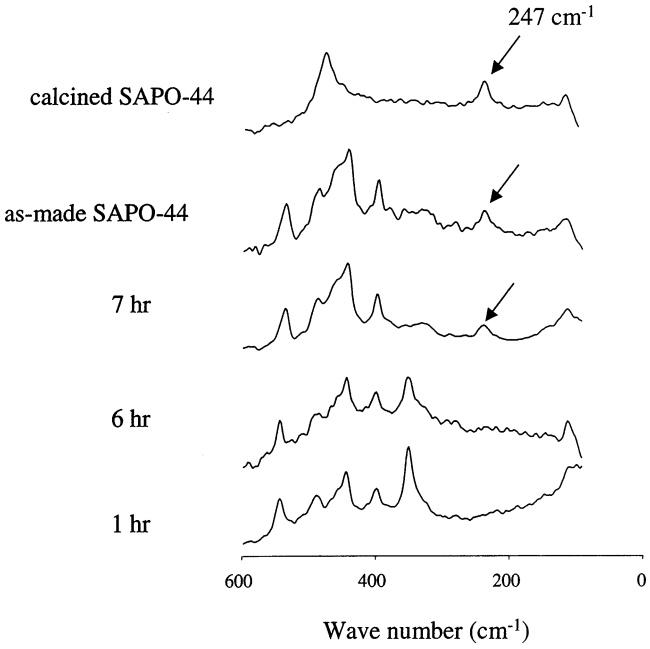

Figure 11. The selected FT-Raman spectra of the gel samples in the frequency range 600−100 cm^{-1}.

be 150.2°. Using the above-mentioned relationship, the frequency of the eight-membered ring breathing mode is predicted to be 249 cm^{-1}, which coincides well with the observed peak at 247 cm^{-1}. Thus, we confidently assign the 247 cm^{-1} peak to the eight-membered ring breathing mode of the SAPO-44 framework. The fact that this peak was not observed in the spectra (Figure 11) of the gel samples heated for less than 7 h suggests that eight-membered rings (therefore the CHA cages) do not exist in either the amorphous or the layered materials. Therefore, the results seem to suggest that the formation of SAPO-44 does not occur through individual CHA cages as building units.

The information regarding the environments around template molecules can also be extracted from the Raman spectra of cyclohexylamine occluded in the solids in the C−H stretching region. As shown in Figure 12, the main difference in spectra between pure cyclohexylamine liquid and the template trapped in SAPO-44 is that, compared to pure liquid, the CH stretching bands of the template trapped inside SAPO-44 moved toward higher energies significantly. For example, the two well-resolved peaks observed at 2937 and 2851 cm^{-1} in the spectrum of pure template liquid shifted to higher frequency by 15 and 14 cm^{-1} to 2952 and 2866 cm^{-1}, respectively, once trapped inside the framework. The XRD results[4] indicated that on average, each ellipsoid CHA cage (about 11 Å long and 6.5 Å wide) contains two template molecules with the cyclohexyl ring being perpendicular to the long axis of the cage (Figure 12) and that these template molecules are tightly trapped inside the cage and cannot be removed by washing or solvent extraction because the size of cyclohexylamine is too large to go through the eight-membered ring window. The observed high-frequency shifts may result from the tight fit of template (kinetic diameter > 6 Å) inside the CHA cage, because the C−H bonds are located

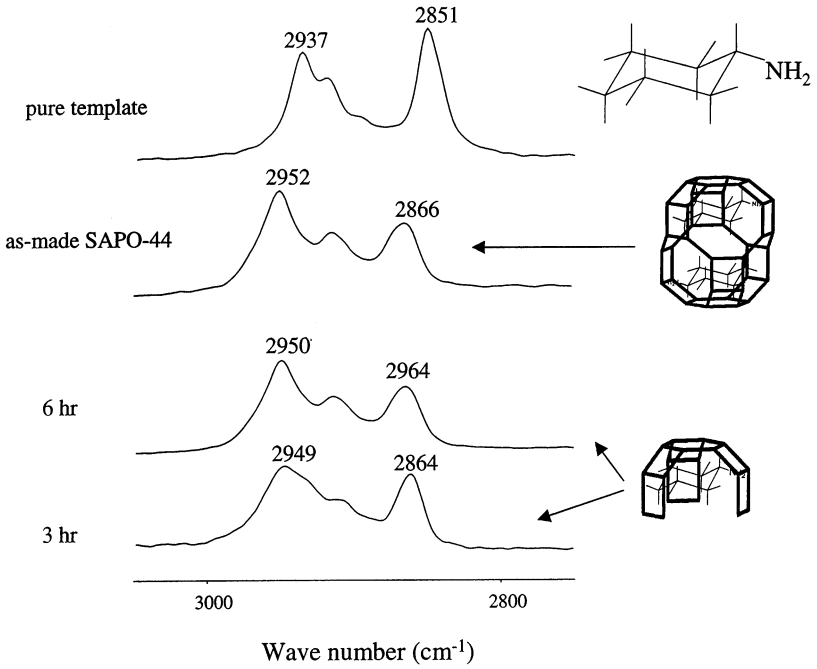

Figure 12. The selected FT-Raman spectra of the gel samples in the C−H stretching region.

on the outside of the molecules and therefore the C−H stretching motions are sensitive to the immediate surroundings. The blue-shift may be interpreted by using an argument put forward by Dutta et al.[25] that the increase in volume of the template during stretching vibrations is resisted by the surrounding of the framework, an effect similar to compression of chemical bonds, which leads to a slight increase in the force constants (C−H bonds are highly anharmonic), resulting in the high frequency shifts. However, in the present case, care must be exercised since the amine molecules occluded inside the cages are likely in the protonated form.[4] It is known that the protonation of amine also causes frequency shift toward higher energies.[26] For this reason, we also obtained the Raman spectrum (not shown) of a protonated cyclohexylamine solution (pH < 2) prepared by acidifying the solution with HCl. Indeed, upon protonation, the C−H modes moved to higher energies. However, the frequencies of the two ν(CH) bands centered at 2936 and 2852 cm^{-1} in the spectrum of pure template only shifted to higher energies by 9 and 7 wavenumbers to 2945 and 2856 cm^{-1}, respectively, and the shift values are smaller than those found for the template trapped inside SAPO-44 (16 and 14 wavenumbers). Apparently, protonation can only account partially for the much larger frequency shift observed in as-made SAPO-44. It seems that the observed changes in frequency for cyclohexylamine contain two different contributions: (1) the confinement imposed by the CHA cages in the SAPO-44 framework, and (2) the protonation of the amine molecules. We have also examined the Raman spectra of the template occluded in the intermediate gel phases. Figure 12 shows that the frequencies of the gel samples heated for 3 and 6 h are close to those of pure SAPO-44, suggesting that the environments of the template molecules in the amorphous and layered materials are very similar to that in SAPO-44 where two cyclohexylamine molecules are trapped inside a CHA cage. As mentioned earlier, CHA cages do not exist in the samples heated for less than 6 h. We suggest that each template molecule may be surrounded by a half CHA cage. A half CHA cage (which does not contain an eight-membered ring) should also impose a restrictive environment similar to that experienced by the template residing inside a whole CHA cage, resulting in the ν(CH) frequencies close to those of cyclohexylamine in SAPO-44.

At this point, we speculate that the formation of SAPO-44 may proceed through the followings: 2 h of hydrothermal treatment mainly generates an amorphous phase consisting of predominately secondary building units such as four-membered ring, six-membered ring, and double six-membered ring. The amorphous phase is AlPO in nature and therefore the secondary building units contain only Al−O−P linkages since ^{29}Si MAS NMR indicates that the Si atoms have not been incorporated into the amorphous material at this stage. After heating the gel for 3 h, the half CHA cages are formed around each cyclohexylamine molecule via assembly of secondary building units and they impose a restricted environment which affects the ν(CH) frequencies of template. The silicon atoms start being incorporated into the amorphous phase at this stage. Heating the gel for 6 h results in joining the half CHA cages to form a layered material (which does not have CHA cages). Further increase in heating time results in the cross link among the layers, leading to the formation of SAPO-44 (which does contain whole CHA cages, therefore 8R).

Summary

In the present work, we have examined the evolution of the gel phases of SAPO-44 synthesis as a function of heating time. The results indicate that the initial gel without heating contains predominately the unreacted Al source. However, as indicated unambiguously by ^{27}Al → ^{31}P CP results, a small amount of AlPO amorphous species does form immediately after mixing the Al and P sources together with template under ambient conditions and the presence of this AlPO species is not immediately apparent from either XRD pattern or simple ^{27}Al and ^{31}P MAS spectra. Hydrothermal treatment of the gel for 2 h yields a solid containing three phosphorus sites. ^{1}H → ^{31}P CP data indicates that these P sites belong to two different domains: (1) an amorphous AlPO species with two P sites that are not fully condensed, and (2) a very small amount of a crystalline AlPO intermediate. The Al−O−P connectivities in each phase are mapped out and the local environment of each

P site probed by $^{27}Al \rightarrow {}^{31}P$ HETCOR experiments. ^{29}Si MAS and $^{27}Al \rightarrow {}^{29}Si$ TEDOR confirm that the silicon atoms only start to incorporate into the AlPO framework after treating the gel at 190 °C for 3 h. Heating the gel for 6 h results in the formation of an SAPO material, which is likely to have a layered structure. This material transforms to SAPO-44 upon further heating. The FT-Raman data indicate that the crystallization does not proceed via the formation of individual CHA cages. The Raman spectra of the template also suggest that the half cages might exist in the intermediate phases. On the basis of the above-mentioned results, a possible route for the formation of SAPO-44 has been suggested.

Acknowledgment. Y.H. acknowledges the financial support from NSERC of Canada for a research and an equipment grant and CFI for the funding for a 400 MHz solid-state NMR spectrometer. Funding from the Canada Research Chair and Primer's Research Excellence Award programs is also gratefully acknowledged. The authors thank Prof. McIntyre and Surface Science Western for the EDX analysis.

Supporting Information Available: Three figures: powder SRD pattern and ^{27}Al MAS spectrum at 4 kHz of aluminum source, Catapal-B; $^{1}H \rightarrow {}^{31}P$ CP intensities as a function of contact times for initial gel and as-made SAPO-44; and ^{27}Al MAS spectrum of as-made SAPO-44 at 6 kHz. This material is available free of charge via the Internet at http://pubs.acs.org.

References and Notes

(1) *Introduction to Zeolite Science and Practice*, 2nd ed.; van Bekkum, H., Flanigen, E. M., Jacobs, P. A., Jansen, J. C., Eds.; Elsevier: Amsterdam, 2001.

(2) Wilson, S. T.; Lok, B. M.; Messina, C. A.; Cannan, T. R.; Flanigen, E. M. *J. Am. Chem. Soc.* **1982**, *104*, 1146.

(3) (a) Gies, H.; Marler, B.; Werthmann, U. In *Molecular Sieves: Science and Technology*; Karge, H. G., Weitkamp, J., Eds.; Springer: Berlin, 1998; Vol. 1, pp 35−64. (b) Davis, M. E.; Lobo, R. F. *Chem. Mater.* **1992**, *4*, 756. (c) Francis, R. J.; O'Hare, D. *J. Chem. Soc., Dalton Trans.* **1998**, 3133. (d) Oliver, S.; Kuperman, A.; Ozin, G. A. *Angew. Chem., Int. Ed. Engl.* **1998**, *37*, 46. (e) Szostak, R. *Molecular Sieves: Principles of Synthesis and Identification*, 2nd ed.; Blackie Academic & Professional: London, 1998. (f) Lobo, R. F.; Zones, S. I.; Davis, M. E. *J. Inclusion Phenom. Mol. Recognit. Chem.* **1995**, *21*, 47. (g) Davis, M. E.; Zones, S. I. *Chem. Industries* **1997**, *69*, 1. (h) Feng, S.; Xu, R. *Acc. Chem. Res.* **2001**, *34*, 239.

(4) Bennett, J. M.; Marcus, B. K. *Stud. Surf. Sci. Catal.* **1988**, *37*, 269.

(5) Wilson, S. T.; Flanigen, E. M. *ACS Symp. Ser. 398*; 1988; 329.

(6) (a) Jeon, J.-K.; Jeong, K.-E.; Park, Y.-K.; Ihm, S.-K. *Appl. Catal. A* **1995**, *124*, 91. (b) Hocevar, S.; Batista, J.; Kaucic, V. *J. Catal.* **1993**, *139*, 351. (c) Lewis, J. M. O.; Price, J. B. U.S. Patent 4,873,390, 1989. (d) Prakash, A. M.; Unnikrishnan, S.; Rao, K. V. *Appl. Catal. A* **1994**, *110*, 1.

(7) (a) Akolekar, D. B.; Bhargava, S. K.; Gorman, J.; Paterson, P. *Colloids Surf., A* **1999**, *146*, 375. (b) Batista, J.; Kaucic, V.; Hocevar, S. *Austr. J. Chem.* **1993**, *46*, 171. (c) Ashtekar, S.; Chilukuri, S. V. V.; Chakrabarty, D. K. *J. Phys. Chem.* **1994**, *98*, 4878. (d) Ashtekar, S.; Chilukuri, S. V. V.; Chakrabarty, D. K. *J. Phys. Chem.* **1996**, *100*, 3665. (e) Olender, Z.; Goldfarb, D.; Batista, J. *J. Am. Chem. Soc.* **1993**, *115*, 1106. (f) Lohse, U.; Parlitz, B.; Altrichter, B.; Jancke, K. *J. Chem. Soc., Faraday Trans.* **1995**, *91*, 1155.

(8) Hing, A. W.; Vega, S.; Schaefer, J. *J. Magn. Reson.* **1992**, *96*, 205.

(9) *Verified Syntheses of Zeolitic Materials*, 2nd ed.; Robson, H., Ed.; Elsevier: Amsterdam, 2001; p 132.

(10) Vega, A. J. *Solid State NMR* **1992**, *1*, 17.

(11) Fyfe, C. A.; Mueller, K. T.; Grondey, H.; Wong-Moon, K. C. *J. Phys. Chem.* **1993**, *97*, 13484.

(12) (a) Davis, M. E.; Monte, C.; Hathaway, P. E.; Garces, J. M. In *Zeolites: Facts, Figures, Future*; Jacobs, P. A., van Santen, R. A., Eds.; Elsevier: Amsterdam, 1989; pp 199−215. (b) He, H.; Klinowski, J. *J. Phys. Chem.* **1994**, *98*, 1192. (c) Prasad, S.; Liu, S. B. *Chem. Mater.* **1994**, *6*, 633. (d) Liu, Z.; Xu, W.; Yang, G.; Xu, R. *Microporous Mesoporous Mater.* **1998**, *22*, 33. (e) Akolekar, D. B.; Bhargava, S. K.; Gorman, J.; Paterson, P. *Colloids Surf.* **1999**, *146*, 375. (f) Jahn, E.; Mueller, D.; Richter-Mendau, J. In *Synthesis of Microporous Materials*; Occelli, M. L., Robson, H. E., Eds.; Van Nostrand Reinhold: New York, 1992; Vol. I, p 248.

(13) (a) Hartmann, P.; Vogel, J.; Schnabel, B. *J. Magn. Reson.* **1994**, *111*, 110. (b) Grimmer, A.-R.; Haubenreisser, U. *Chem. Phys. Lett.* **1983**, *99*, 487. (c) Mudrakovskii, I. L.; Shmachkova, V. P.; Kotsarenko, N. S.; Mastikhin, V. M. *J. Phys. Chem. Solids* **1986**, *47*, 335.

(14) (a) Sayari, A.; Moudrakovski, I.; Reddy, J. S.; Ratcliffe, C. I.; Ripmeester, J. A.; Preston, K. F. *Chem. Mater.* **1996**, *8*, 2080. (b) Blackwell, C. S.; Patton, R. L. *J. Phys. Chem.* **1988**, *92*, 3965. (c) Hasha, D.; Sierra de Saldarriaga, L.; Saldarriaga, C.; Hathaway, P. E.; Cox, D. F.; Davis, M. E. *J. Am. Chem. Soc.* **1988**, *110*, 2127.

(15) Ren, X.; Komarneni, S.; Roy, D. M. *Zeolites* **1991**, *11*, 142.

(16) Pines, A.; Gibby, M. G.; Waugh, J. S. *J. Chem. Phys.* **1973**, *59*, 569.

(17) (a) Vega, A. J. *J. Am. Chem. Soc.* **1988**, *110*, 1049. (b) Fyfe, C. A.; Zhang, Y.; Aroca, P. *J. Am. Chem. Soc.* **1992**, *114*, 3252.

(18) Fyfe, C. A.; Woon-Moon, K. C.; Huang, Y.; Grondey, H.; Mueller, K. T. *J. Phys. Chem.* **1995**, *99*, 8707.

(19) Harris, R. K. *Analyst* **1985**, *110*, 649.

(20) Maciel, G. E.; Sindorf, D. W. *J. Am. Chem. Soc.* **1980**, *102*, 7606.

(21) Barrie, P. J. In *Spectroscopy of New Materials*; Clark, R. J. H., Hester, R. E., Eds.; John Wiley & Sons: Chichester, 1993; pp 151, and references therein.

(22) Fyfe, C. A.; Wong-Moon, K. C.; Huang, Y. *Zeolites* **1996**, *16*, 50.

(23) (a) Dutta, P. K.; Shieh, D. C.; Puri, M. *Zeolites* **1988**, *8*, 306. (b) Creighton, J. A.; Deckman, H. W.; Newsam, J. M. *J. Phys. Chem.* **1991**, *95*, 2099. (c) Dutta, P. K.; Rao, K. M.; Park, J. Y. *J. Phys. Chem.* **1991**, *95*, 6654.

(24) Holmes, A. J.; Kirby, S. J.; Ozin, G. A.; Young, D. *J. Phys. Chem.* **1994**, *98*, 4677.

(25) Dutta, P. K.; Shieh, D. C.; DelBarco, B. *Chem. Phys. Lett.* **1986**, *127*, 200.

(26) Popescu, S. C.; Thomson, S.; Howe, R. F. *Phys. Chem. Chem. Phys.* **2001**, *3*, 111.